International Journal of Concrete Structures and Materials
Vol.9, No.3, pp.307–321, September 2015
DOI 10.1007/s40069-015-0110-y
ISSN 1976-0485 / eISSN 2234-1315

# Automated Surface Wave Measurements for Evaluating the Depth of Surface-Breaking Cracks in Concrete

**Seong-Hoon Kee[1),*], and Boohyun Nam[2)]**

(Received February 2, 2015, Accepted August 12, 2015, Published online September 2, 2015)

**Abstract:** The primary objective of this study is to investigate the feasibility of an innovative surface-mount sensor, made of a piezoelectric disc (PZT sensor), as a consistent source for surface wave velocity and transmission measurements in concrete structures. To this end, one concrete slab with lateral dimensions of 1500 by 1500 mm and a thickness of 200 mm was prepared in the laboratory. The concrete slab had a notch-type, surface-breaking crack at its center, with depths increasing from 0 to 100 mm at stepwise intervals of 10 mm. A PZT sensor was attached to the concrete surface and used to generate incident surface waves for surface wave measurements. Two accelerometers were used to measure the surface waves. Signals generated by the PZT sensors show a broad bandwidth with a center frequency around 40 kHz, and very good signal consistency in the frequency range from 0 to 100 kHz. Furthermore, repeatability of the surface wave velocity and transmission measurements is significantly improved compared to that obtained using manual impact sources. In addition, the PZT sensors are demonstrated to be effective for monitoring an actual surface-breaking crack in a concrete beam specimen subjected to various external loadings (compressive and flexural loading with stepwise increases). The findings in this study demonstrate that the surface mount sensor has great potential as a consistent source for surface wave velocity and transmission measurements for automated health monitoring of concrete structures.

**Keywords:** surface waves, surface wave transmission, surface-breaking crack, concrete, non-destructive evaluation.

## 1. Introduction and Motivation

Surface wave measurements have been widely used to develop non-destructive evaluation (NDE) techniques for concrete structures in civil engineering due to their useful features (Graff 1991). Surface waves are mechanical waves that propagate along the surface of concrete with most of their energy confined near the surface, which enables one-sided access of concrete structures. The particle vibration amplitude of surface waves exponentially decreases with distance from the free surface boundary and with a frequency-dependent penetration depth, which is particularly useful to identify and characterize surface-breaking or subsurface defects in concrete structures (Achenbach 2000, 2002). In infinite media, surface waves are non-dispersive, that is the wave velocity does not change with frequency. In practice, this assumption is valid when the thickness $H$ of the solid body of interest is sufficiently larger than the wavelength $\lambda$ of the surface wave (i.e., $H > 2\lambda$). In thin plates or layered systems, the velocity of surface wave changes with frequency. Surface wave velocity measurements have been demonstrated to be effective for characterizing mechanical properties of concrete in many civil engineering applications (ACI committee 228 1998).

In surface wave measurements, an impact source is used to generate incident surface waves, and two receivers are used to measure the surface waves propagating in concrete (see Fig. 1). Selecting an appropriate impact source is of great importance for successfully measuring surface waves in concrete structures. The normal impact of a ball on the concrete surface has been widely used as a source for surface wave-based NDE techniques. According to the Hertzian impact theory (McLaskey and Glaser 2010), the impulse force (or force pulse) is approximated by a "half sine" pulse, and the duration of the pulse depends on the geometry and material properties of a ball and a massive material that the ball hits; however, the most influential factor is the radius of the ball. Therefore, the correct ball size can be selected so that the frequency bandwidth generated by the impact source appropriately covers a frequency range of interest for the surface wave measurements. In practice, the impact source is usually operated by hand; however, there are several limitations to this method. First, it is difficult to generate consistent waves with an impact source controlled by a human hand. Furthermore, it is impossible to conduct surface wave

[1)]Department of Architectural Engineering, Dong-A University, Busan 604-714, Korea.
*Corresponding Author; E-mail: shkee@dau.ac.kr
[2)]Department of Civil, Environmental and Construction Engineering, University of Central Florida, Orlando, FL 32816, USA.

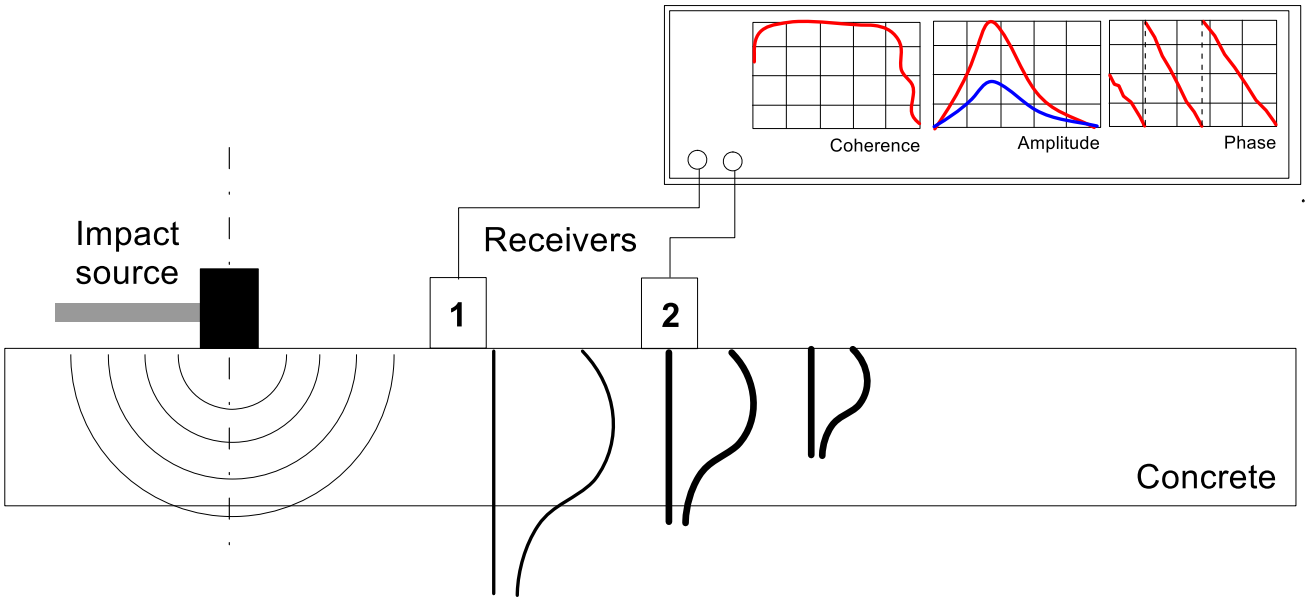


**Fig. 1** Source and receiver configuration for surface wave measurements.

measurements in hard-to-access regions of concrete structures, due to safety reasons or spatial limitations. Regardless of the feasibility of these methods, it would be time and labor intensive to be used in large civil structures.

A possible solution to the aforementioned problems can be obtained by using "surface-mounted piezoelectric transducers (PZT)". PZT has been successfully applied to the structural health monitoring of concrete structures by using stress wave-based methods (Liao et al. 2011; Okafor et al. 1996; Song et al. 2006). The wave propagation properties were studied to detect and evaluate the cracks and damages inside concrete structures. Wang et al. (2001) studied the debonding behavior between steel rebar and concrete by using PZT (lead zirconate titanate) patches fixed to generate and receive elastic waves in concrete, and obtained the modulus of elasticity by utilizing the wave propagation characteristics. Song et al. (2007, 2008) developed smart aggregates to perform structural health monitoring for concrete structures. The mortar-typed aggregate was embedded in concrete structures during casting and successfully used for monitoring damage in concrete structures by measuring an energy-based damage index. Dong et al. (2011) developed a cement-based piezoelectric ceramic composite and effectively applied it as a sensor for health monitoring of concrete structures. Hou et al. (2012, 2013) developed a marble-based smart aggregate for seismic compressive and shear stresses. Recently, Kee and Zhu (2013) developed PZT embedded sensors using a PZT disc that can be used as ultrasonic transmitting and receiving transducers for ultrasonic pulse velocity tests. In this study, the author developed a surface-mount sensor using a PZT disc for generating incident surface waves for surface wave velocity and transmission measurements in concrete structures.

The primary objective of this study is to investigate the feasibility of an innovative surface-mount sensor made of a PZT disc (hereafter refer to as "surface-mount sensor") as a consistent source for surface wave velocity and transmission measurements in concrete structures. Two surface-mount sensors were attached to a concrete slab with dimensions of 1500 by 1500 by 200 mm (width X length X thickness). The slab possessed a surface-breaking crack located in the middle of the slab, which extended to varying depths. Two surface-mount sensors on either side of the surface-breaking crack worked as actuators driven by an ultrasonic pulse-and-receiver, and two accelerometers worked as a receiver. A series of surface wave measurements was performed to investigate the performance of the surface-mount sensors as a consistent source. An additional aspect to the investigation was to test the ability of surface-mount sensors to perform automated monitoring of an actual surface-breaking crack in a concrete beam subjected to various external loadings (compressive and flexural loading with stepwise increasing) (ElSafty and Abdel-Mohti 2013; Soltani et al. 2013).

## 2. Background

### 2.1 Ultrasonic Surface Waves (USW) Method

The surface wave velocity methods involve determining the relationship between the wavelength and velocity of surface vibrations at varying vibration frequencies. The resulting relation is called a dispersion curve, which is generally determined by the spectral analysis of surface waves (SASW) (Nazarian and Desai 1993; Nazarian and Stokoe 1986). For plate-like concrete structures (deck, slab, wall, etc.), the ultrasonic surface wave (USW) technique has been demonstrated to be effective for evaluating material damages caused by many sources: ASR, DEF, freeze-and-thaw, and corrosion of reinforcing steel (Gucunski et al. 2013). The USW test consists of recording the response of the concrete, at two receiver locations, to an impact on the surface of the concrete in structures (See Fig. 1). The surface wave velocity can be obtained by

measuring the phase difference $\Delta\Phi$ between two different sensors (sensor 1 and sensor 2) ($C = 2\pi fd/\Delta\Phi$; where $f$ is frequency, and $d$ is the distance between two sensors). The frequency range of interest in the USW technique is a high-frequency range compared to the thickness of the tested object, in which surface waves are non-dispersive. In cases of relatively homogeneous materials, the velocity of the surface waves does not vary significantly with frequency. Therefore, the surface wave velocity can be precisely related to the elastic modulus of concrete, using the measured or assumed mass density and Poisson's ratio of the material. A complex process called inversion is not necessary in the USW technique, leading to a substantially reduced time required for data interpretation and post-processing. In the case of a sound and homogenous concrete plate, the velocity of the surface waves will show little variability, while significant variation in the phase velocity will be an indication of the presence of a defect or other anomaly.

### 2.2 Surface Wave Transmission (SWT) Method

The surface wave transmission (SWT) method has been demonstrated to be effective for evaluating surface-breaking or sub-surface defects in concrete structures. The SWT method uses the frequency-dependent penetration depth of surface waves. When incident surface waves ($R_i$) propagate across a surface-breaking crack, the low-frequency components of the incident surface waves will transmit to the forward scattering field with attenuation ($R_{tr}$), while the high-frequency components will reflect back ($R_r$). Consequently, the transmission coefficient of surface waves $Tr$ across a surface-breaking crack, which is defined as the ratio of spectral amplitudes of $R_{tr}$ to $R_i$, depends on the frequency of surface waves and dimensions of the defect in the concrete. For example, an analytical solution relating $Tr$ and the normalized crack depth ($h/\lambda$, $h$ is the depth of a surface-breaking crack) was given by Achenbach and his colleagues (Achenbach et al. 1980; Angel and Achenbach 1984; Mendelsohn et al. 1980). It was demonstrated through numerical simulations and experimental studies that the SWT method is effective for evaluating the depth of surface-breaking cracks in concrete structures (Hevin et al. 1998; Kee 2011; Kee and Zhu 2011; Popovics et al. 2000; Shin et al. 2008; Song et al. 2003). Test configuration of the SWT method is the same as that of the USW method, consisting of two receivers and an impact source. However, the measured amplitude of the surface waves is sensitive to the coupling condition of the sensors and the magnitude of impact force, which may cause significant errors in predicted values. It has been demonstrated that the self-calibrating procedure is effective for eliminating undesirable effects due to sensors and sources in the SWT method (Popovics et al. 2000). Recently, Kee and Zhu (2011, 2010) proposed the air-coupled sensing method, which significantly improves signal consistency and test speed in transmission measurements of surface waves in concrete.

### 2.3 Preparation of Piezoelectric Sensor

A piezoelectric sensor is an active element that converts electrical energy to mechanical energy, and mechanical energy to electrical energy (i.e., the piezoelectricity). The piezoelectricity causes a sensor to produce electric charges when subjected to stress (receiving action) and conversely, to generate mechanical vibrations when an electrical voltage is applied (actuator action). In this study, a piezoelectric disc is used as an actuator for generating incident surface waves in concrete.

A piezoelectric disc is one of the most widely used piezoelectric elements, as shown in Fig. 2. The thickness of a piezoelectric disc is much smaller than its lateral dimensions. The sensors used in this study are commercial piezoelectric warning devices, which generate sound when a voltage is applied continuously. One side of the piezoelectric element is attached to a metal plate (brass) for reinforcing the thin piezoelectric disc. A piezoelectric disc is polarized in the thickness direction. In the actuating mode, the disc expands/contracts in the thickness direction, i.e., along the axis of polarization, when a voltage is applied to the two surfaces of the ceramic disc, as shown in Fig. 2b. At the same time, the disc contracts/expands in the transverse direction. In the receiving mode, mechanical vibrations generate electric charges in the piezoelectric disc.

Two piezoelectric sensors were attached to the concrete surface to generate incident surface waves in concrete structures. The piezoelectric disc has a thickness of 0.2 mm (7.87 mils) and a diameter of 22 mm (866.14 mils). Two wires were then soldered to the electrodes on the piezoelectric disc. Since concrete surfaces are often under conductive environments, electrical shielding and waterproofing were needed. The waterproof procedure follows the description given by Jung (Jung 2005). First, five layers of polyurethane coating (M-coat A by VISHAY®) were applied to the surface of the piezoelectric discs. Each coating had to be fully air-dry before applying a subsequent one.

## 3. Experimental Program

### 3.1 Preparation of Specimens

Two concrete specimens were prepared in the laboratory to investigate the performance of the surface-mount sensor as an impact source in surface wave measurements. One concrete specimen (specimen 1) prepared in the laboratory had lateral dimensions of 1500 mm$^2$ and a thickness of 200 mm (see Fig. 3). A notch-type crack was made at the mid-section of the specimen by inserting a 0.5 mm thick Zinc sheet before pouring the concrete. The notch-type crack was designed to have depths increasing stepwise from 10 to 100 mm, at intervals of 10 mm (Fig. 3b). The Zinc sheet was coated by a thin plastic film to avoid chemical bonding between the Zinc sheet and concrete during the cement hydration process, and to facilitate the extraction of the sheet from the concrete. The Zinc sheet was removed about 6 h after casting, slightly earlier than the final setting of the

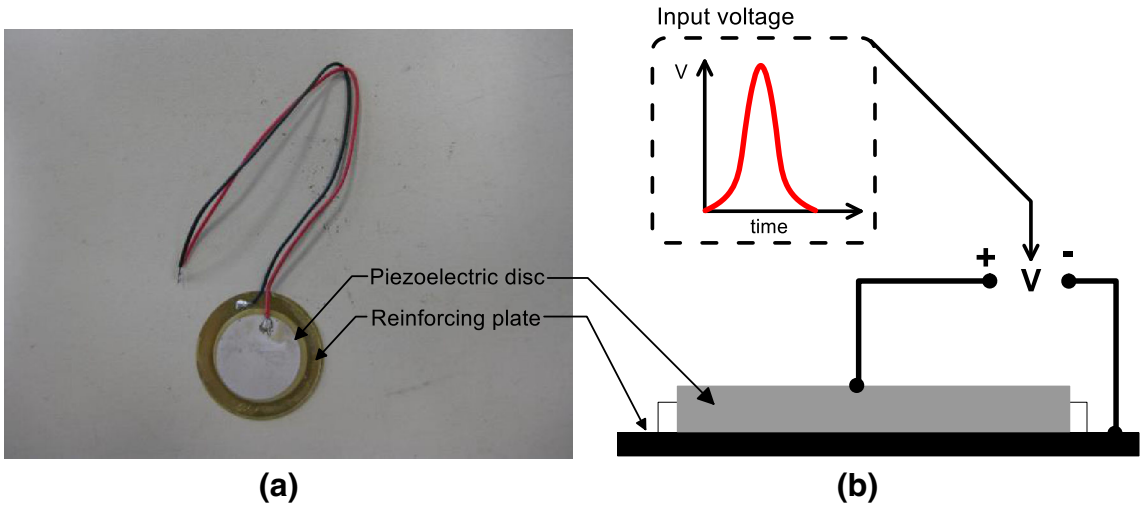


**Fig. 2** Structure of piezoelectric disc sensor: **a** a photo of the piezoelectric disc, and **b** a piezoelectric disc connected to a voltage.

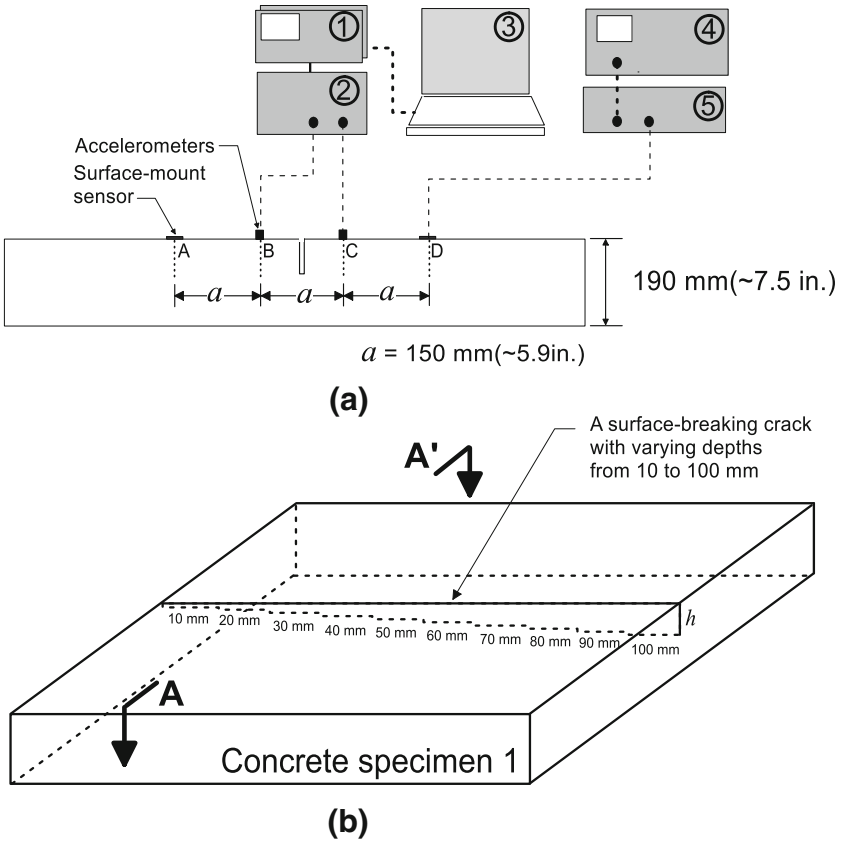


**Fig. 3** Sectional view of a concrete slab (specimen 1), and data acquisition and signal generation systems for surface wave measurement using surface-mount sensors (**a**), and **b** isometric view of the concrete specimen 1.

concrete, based on observations from a series of preliminary tests before fabricating the actual specimen. Finally, the width of the crack in the hardened concrete specimen, measured with a crack width gauge after 7 days, was approximately 0.5 mm. The proposed surface-mount sensors were attached on either side of the notch crack (see Fig. 3a). Concrete material used for specimen 1 was normal weight, ready-mixed concrete made of type I/II cement, river sand, and coarse aggregate with a maximum size of 19 mm. The design compressive strength of concrete was 20 MPa. Compressive strength measured according to ASTM C39 (ASTM C39 2014) at the time of testing ranges from 22.4 to 24.3 MPs, with a mean value of 23.58 MPa. P wave velocities measured with a pair of 54 kHz ultrasonic transducers in the through-transmission mode were in the range of 4331 and 4386 m/s.

In addition, a concrete beam (specimen 2) with dimensions of 400 by 1500 mm and a thickness of 190 mm was prepared in the laboratory, as shown in Fig. 5. Concrete used for the specimen 2 was normal weight, ready-mixed concrete made from Type I/II cement, river sand, and coarse aggregate with a maximum size of 19 mm. The design compressive strength of

the concrete was 20 MPa. Three cylinder specimens were used to measure concrete compressive strength according to ASTM C39 (ASTM C39 2014), resulting in a measured compressive strength (at the time of testing) ranging from 22.3 to 25.58 MPa, with a mean value of 22.84 MPa. P-wave velocities measured with a pair of 54 kHz ultrasonic transducers were in the range of 4328 and 4375 m/s.

Two layers of longitudinal reinforcing bars (13.3 mm diameter) were used for the top and bottom layers, respectively. A real surface-breaking crack was designed to appear in the middle of the concrete specimen by three-point bending (see Fig. 4a). Before applying external loadings, two proposed surface-mount piezoelectric sensors were attached to the concrete on either side of the expected crack location. To ensure generation of a single flexural crack in the middle of the concrete specimen, the reinforcing bars were unbonded to the concrete by wrapping a thin, 400 mm-long plastic film around the middle section of the reinforcing bars. After cracking, it is reasonable to assume that concrete in the crack section cannot provide any tensile strength, and only the top reinforcing bars participate in the load-resistance mechanism. Assuming a constant strain distribution in the unbonded steel reinforcing bars, shear stresses in the unbonded concrete region disappear after cracking, which prevents initiation of additional shear cracks or other flexural cracks in the middle of the concrete specimen. Consequently, a single vertical surface-breaking crack will occur in the middle section of the specimen. In addition, transverse reinforcing bars (No. 3) were placed to avoid abrupt shear failure and to ensure flexural failure of the beam.

### 3.2 Surface Wave Measurements

The test setup for surface wave measurements using surface-mount sensors consists of a function generator, a power amplifier, a pair of surface-mount sensors and accelerometers (as sources and receivers, respectively), a digital oscilloscope, a computer, and LabVIEW program (see Figs. 4a, 5a). The two surface-mount sensors were located at A and D, and two accelerometers (PCB 352C65) were located at B and C on concrete specimens 1 and 2 (see Figs. 3a, 4a). A function generator (EXTX/2A60) was used to drive the surface-mount sensors. Stress waves are highly attenuated as they propagate through concrete. Therefore, a power amplifier (Trek PZD250) was used to amplify the signal generated by the function generator. Gaussian functions with a duration T of 100 μs were used as an input signal for the function generator. The acquired signals were digitized by a high-speed digital oscilloscope (NI-PXI 5101) at a sampling frequency of 1 MHz and total signal length of 0.001 s. The digitized data were then transferred to a laptop computer for data storage and post-processing. To eliminate the effects of experimental variations regarding sensor and source, the

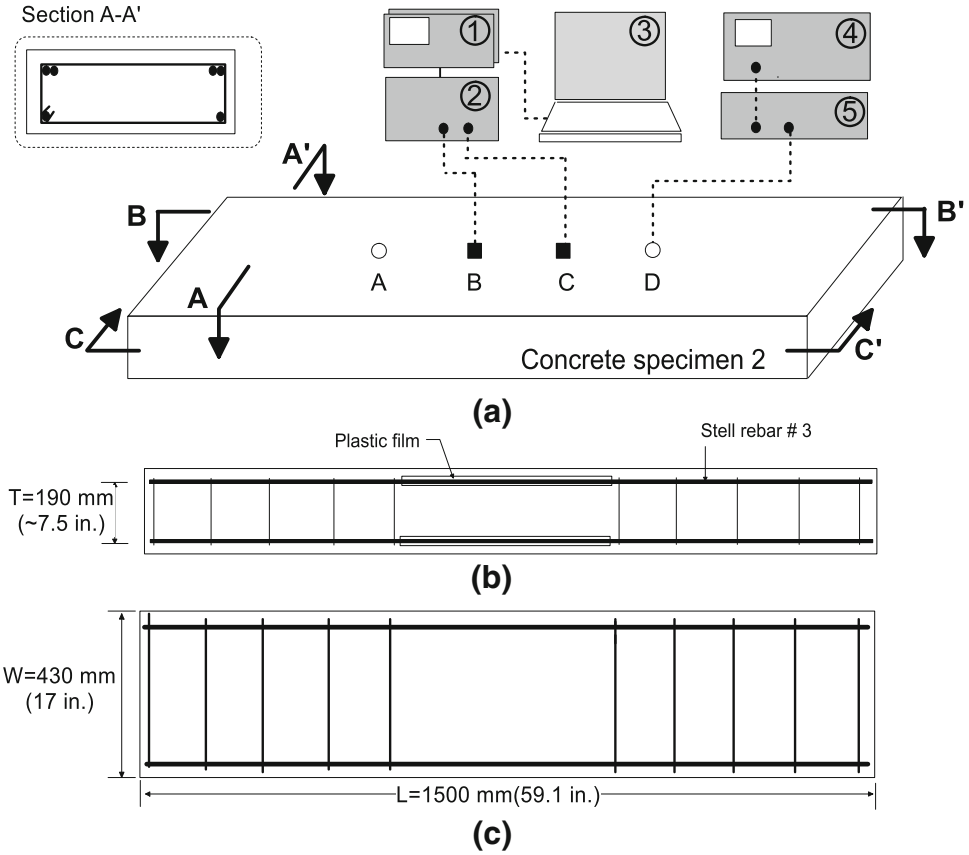


**Fig. 4** Isometric view of a concrete beam (specimen 2), and data acquisition and signal generation systems for surface wave measurement using surface-mount sensors (**a**), sectional view of the specimen 2 (*B*-*B*′), and (**c**) sectional view of the specimen 2 (*C*–*C*′).

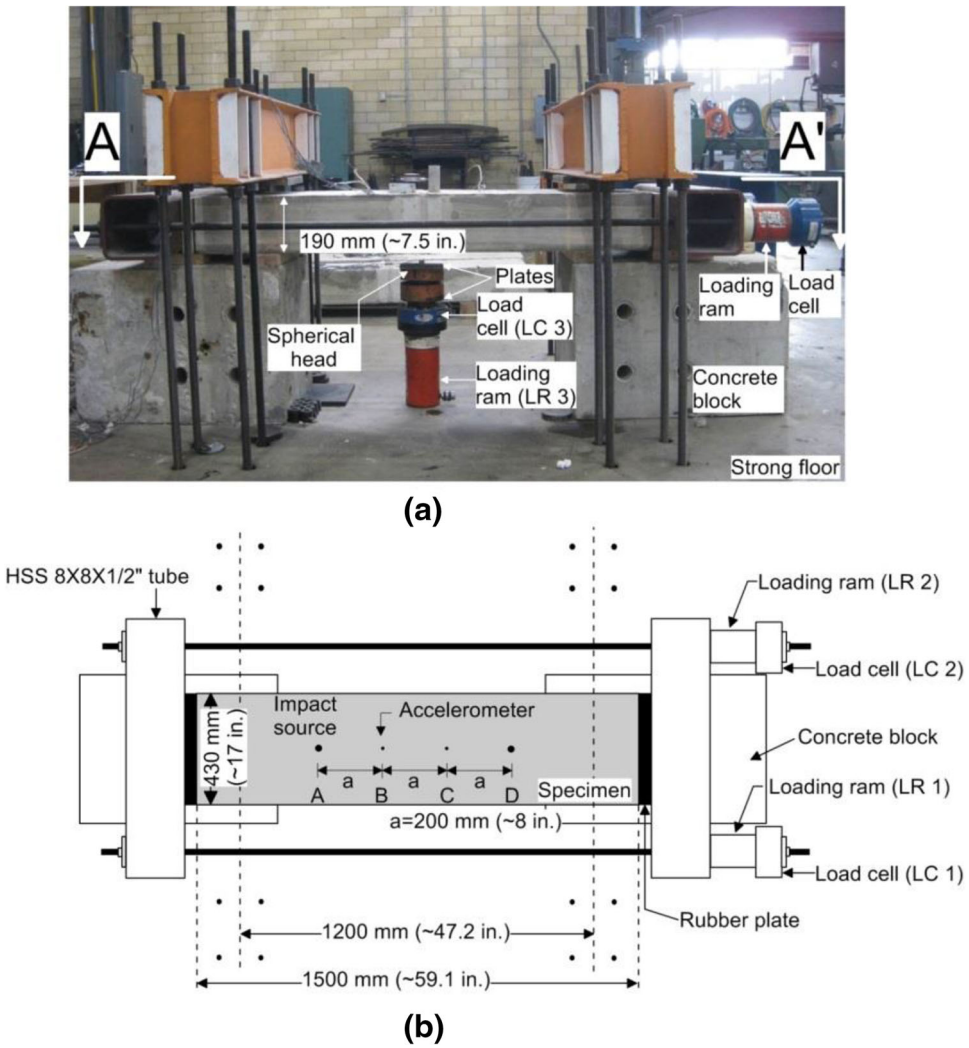


**Fig. 5** Test setup of a concrete beam (specimen 2) for applying compressive forces and generating a single surface-breaking crack: **a** a photo of a test setup, and **b** plan view from the section $A$-$A'$ shown in (**a**).

self-calibrating procedure (Popovics et al. 2000) was used to measure surface wave transmission and velocity. Two accelerometers were placed at locations B and C of the test specimens 1 and 2 to measure surface waves. First, the stress waves generated by the impact source at A propagated towards the sensor at B, and then towards the far sensor at C, denoted as $\mathbf{V}_{AB}$, and $\mathbf{V}_{AC}$, respectively. For example, the typical time signals $\mathbf{V}_{AB}$ and $\mathbf{V}_{AC}$ measured across a surface-breaking crack with a 20 mm depth in the specimen 1 are shown in Fig. 6a. Surface wave components were extracted from the full waveform in time domain by applying a hanning window (bold lines in Fig. 6a), and converted to frequency domain signals, denoted as $\mathbf{S}_{AB}$, and $\mathbf{S}_{AC}$ respectively. Similarly, stress waves generated by the surface-mount sensor at D were measured by accelerometers at C and B, denoted as $\mathbf{S}_{DC}$ and $\mathbf{S}_{DB}$. The frequency domain signals of $\mathbf{S}_{AB}$, $\mathbf{S}_{AC}$, $\mathbf{S}_{DC}$ and $\mathbf{S}_{DB}$ were used to calculate the transmission functions of surface waves propagating through the cracked region BC in concrete specimens ($\mathbf{S}_{AC}/\mathbf{S}_{AB}$ and $\mathbf{S}_{DB}/\mathbf{S}_{DC}$). The modulus (amplitude) and phase angle of the transmission functions are shown in Fig. 6b, c, respectively. In the cracked region, the phase angle of $\mathbf{S}_{AC}/\mathbf{S}_{AB}$ (or $\mathbf{S}_{DB}/\mathbf{S}_{DC}$) almost linearly increases in a frequency range between 0 and about 45 kHz, in which the slope of the phase spectra is comparable to the theoretical value of the solid concrete with the surface wave velocity of 2200 m/s. In contrast, the modulus of $\mathbf{S}_{AC}/\mathbf{S}_{AB}$ (or $\mathbf{S}_{DB}/\mathbf{S}_{DC}$) decreases with increasing frequency, which is clearly differentiated from the theoretical curve of the solid concrete. Therefore, it can be seen that the modulus components of the transmission function are more informative of the presence and characteristics of surface-breaking cracks in concrete then the phase components.

In this study, the surface wave transmission ratio between B and C was calculated by averaging signals in the frequency domain obtained from opposite sides according to the self-calibrating procedure (Popovics et al. 2000) as follows,

$$\mathbf{Tr}_{BC} = \sqrt{\frac{\mathbf{S}_{AC}\mathbf{S}_{DB}}{\mathbf{S}_{AB}\mathbf{S}_{DC}}} \tag{1}$$

In this study, five repeated signal data sets were collected at the same test location to investigate the repeatability of signals generated by the surface-mount sensors. The transmission coefficient measured from cracked regions was further normalized by the reference, producing the

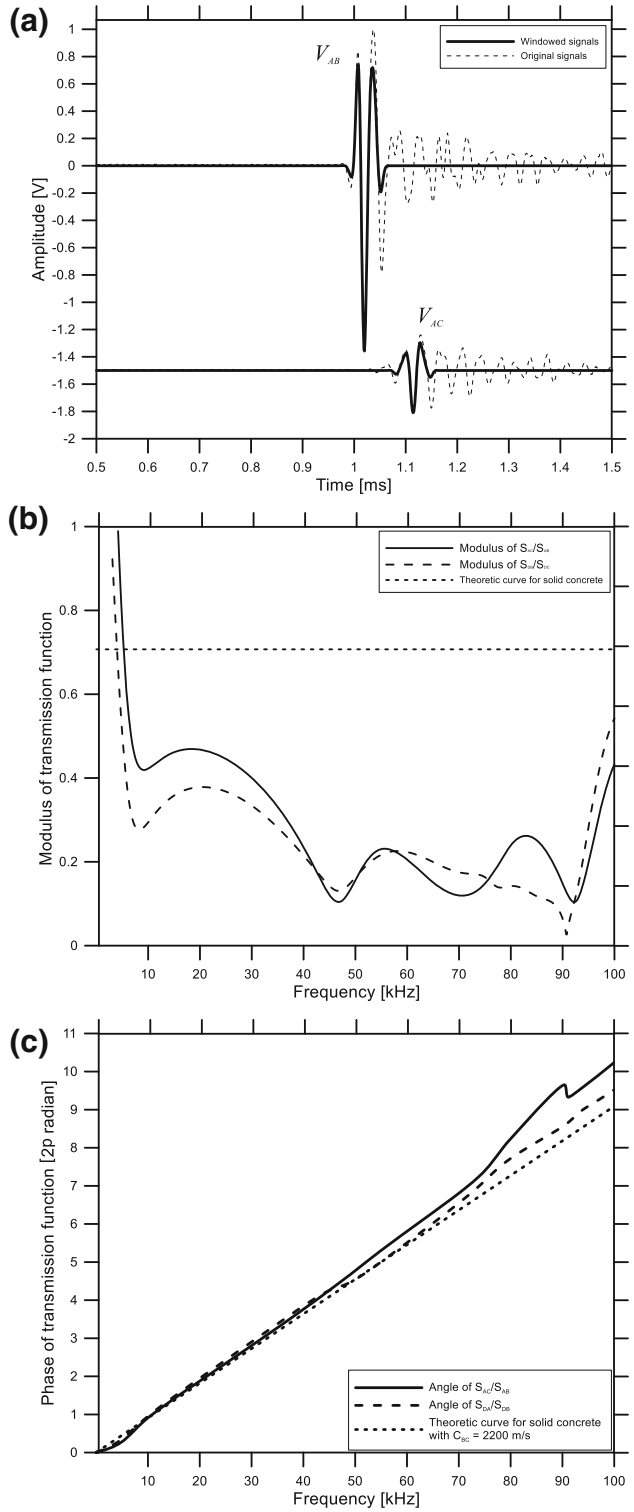


**Fig. 6** Typical signals generated by the surface-mount piezoelectric transducers, measured using accelerometers across a surface breaking crack with a depth of 20 mm in the specimen 1: **a** time signals, **b**, **c** the modulus and phase angle of the transmission functions ($S_{AC}/S_{AB}$ or $S_{DB}/S_{DC}$).

normalized transmission coefficient $\mathbf{Tr}_n$. It has been demonstrated that effects due to geometric attenuation and material damping can be effectively reduced by using the normalization process.

The phase velocity of the surface wave was calculated in the frequency domain by using the spectral analysis of surface waves (SASW). First, the phase difference between $\mathbf{S_{AB}}$ and $\mathbf{S_{AC}}$ by a source at A ($\phi_{BC}$) and between $\mathbf{S_{DC}}$ and $\mathbf{S_{DB}}$ by a source at D ($\phi_{CB}$) was calculated. Then the average phase velocity $\mathbf{C}_{BC}$ was calculated using the average phase difference as follows,

$$\mathbf{C}_{BC} = 2\pi f \frac{BC}{(\phi_{BC} + \phi_{CB})/2} \tag{2}$$

where BC is the distance between two sensors on the locations B and C in Figs. 3, 4, 5 (BC = 200 mm in this study).

## 4. Results and Discussion

### 4.1 Repeatability of Signals Generated by the Surface-Mount Sensors

In this study, the repeatability of measured signals generated by the piezoelectric sensors was evaluated by the coherence function as follows,

$$\gamma_j(f) = \frac{\left|\sum_{i=1}^{5} \mathbf{P}_{1j}^{i}(f)\right|}{\sqrt{\sum_{i=1}^{5} \mathbf{P}_{11}^{i}(f) \times \sum_{i=1}^{5} \mathbf{P}_{jj}^{i}(f)}} \tag{3}$$

where $\mathbf{P}_{1j}^{i}(f)$ is the cross-power spectrum of the reference signal and the signal measured at the $j$th test step; $\mathbf{P}_{11}^{i}(f)$ and $\mathbf{P}_{jj}^{i}(f)$ represent the auto-power spectrum of these signals; $i$ is the index of the five repeated time domain signals; and $f$ is frequency. The coherence function represents the degree of correlation between two signals as a function of frequency. The resulting $\gamma$ ranges from 0 to 1.0, in which a value close to 1.0 indicates a good signal coherence. There are several factors that makes the coherence function less than one, including (i) measurements with incoherent noise, (ii) inconsistent coupling of source-and-receiver transducer and (iii) additional inputs in materials (i.e., additional scattering by any changes in internal defects).

Figure 7a shows the signal coherence $\gamma$ of the measured signals generated by the surface-mount sensors on a crack-free region in specimen 1. For comparison purposes, the coherence curve of signals generated by a manual impact source (a steel ball of 13 mm diameter) is shown as a dash line in Fig. 6. It is demonstrated that the piezoelectric surface-mount sensors produce a very repeatable signal in a wideband frequency range of 0–100 kHz where $\gamma \geq 0.999$, a criterion for a useful frequency range in this study. In contrast, the measured signals generated by a manual impact source shows good signal consistency in the frequency range of 10–30 kHz: the useful frequency range depends on the diameter of the steel ball used for impact sources.

It is also observed that the presence of a surface-breaking crack decreases the magnitude of $\gamma$ in high-frequency ranges: the useful frequency range becomes narrower as the depth of a crack increases from 0 to 50 mm (see Fig. 7b). However, it is not necessarily attributed to the coupling

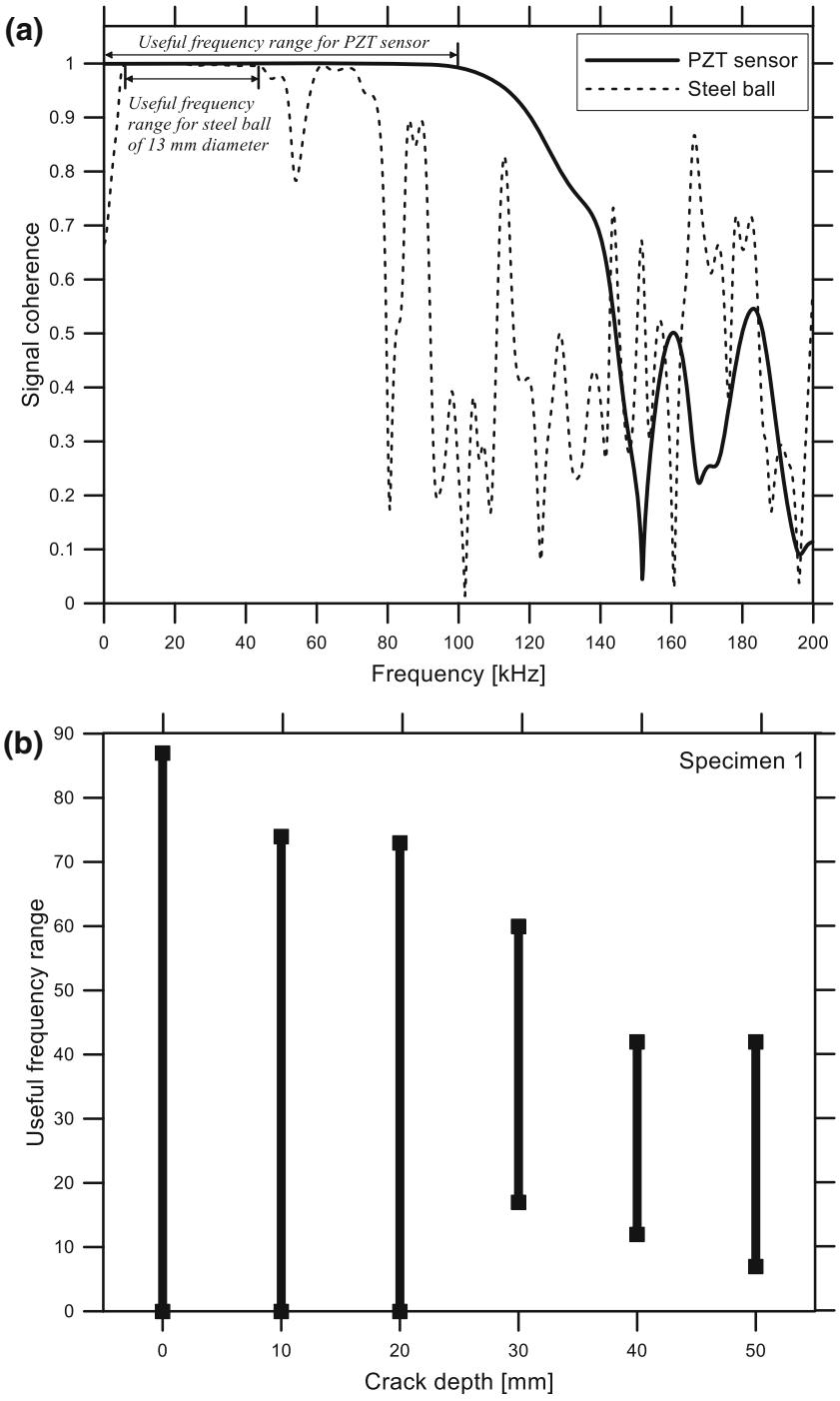


**Fig. 7** Comparison of signal coherence generated by the surface-mount transducers and manual impact sources (**a**), and variations of the useful frequency range in a signal coherence function with increasing depth of the surface-breaking crack in concrete (**b**).

performance of the surface-mount sensor because the surface-breaking crack does not affect the surface-mount source and accelerometers. Instead, this phenomenon can be explained by the fact that the high-frequency components of surface waves are reflected back to the backward scattering field: consequently, the presence of a surface-breaking crack can significantly decrease the energy of transmitted surface waves in a higher frequency range.

### 4.2 Consistency of the Measured Surface Wave Parameters (Velocity and Transmission)

The consistency of measured results is of great interest when exploring the performance of surface-mount sensors. Ten repeated surface wave measurements were conducted at each test step using the same test setup and data acquisition system, in which surface-mount sensors located at A and D were alternatively used for generating incident waves in

concrete. At each test step, the velocity and transmission coefficient of surface waves were determined by using Eqs. 1 and 2, respectively. In this study, the coefficient of variation (COV, the standard deviation divided by the mean value of a set of samples) was used as a means of consistency for the resulting surface wave velocity and transmission coefficients.

Figure 8a shows COVs of the two sets of surface wave transmission coefficients ($Tr_{PZT}$ and $Tr_{SB}$) measured in the crack-free region of specimen 1. The COVs of $Tr_{PZT}$ and $Tr_{SB}$ remain low and flat, with values of 1.24 ± 0.39 % (μ ± σ) and 2.29 ± 0.65 % (μ ± σ) in a useful frequency range for each method (i.e., 0–100 kHz for $Tr_{PZT}$ and 10 kHz to 30 kHz for $Tr_{SB}$), where μ and σ are the mean value and the standard deviation of COV, respectively. Similarly, the COVs of the phase velocity of surface waves ($C_{R,PZT}$ and $C_{R,SB}$) are shown in Fig. 8b. The COVs of $C_{R,PZT}$ and $C_{R,SB}$ are 0.04 ± 0.023 % (μ ± σ) and 0.3 ± 0.15 %, respectively, in the useful frequency range of each method. Therefore, Fig. 8 illustrates that the surface-mount sensors produce equivalent or improved consistency of surface wave transmission and velocity measurements compared to the measurements using a manual impact source.

Furthermore, it is observed that the presence of a surface-breaking crack may affect the COV of both the $Tr_{PZT}$ and $C_{RPZT}$ (Fig. 9). For specimen 1, the COVs of $Tr_{PZT}$ and $C_{RPZT}$ gradually increase up to 5 and 4 %, compared to reference values measured on the crack-free region where crack depth increases from 0 to 50 mm. For test specimen 2, the COVs of $Tr_{PZT}$ and $C_{R,PZT}$ at 20 kHz in the crack-free surface are 1.2 and 0.01 %, respectively. However, onset of a surface-breaking crack in the middle of the concrete (a depth of about 150 mm) significantly increases the COVs of $Tr_{PZT}$ and $C_{R,PZT}$ to about 10 and 3 %, respectively. It appears that higher variability in cracked concrete is due to a combination of two reasons: (i) energy loss of transmitted surface waves due to a surface-breaking crack, and (ii) scattering of the surface wave at the tip of the crack. However, as will be demonstrated in the next section, the COV levels of $Tr_{PZT}$ and $C_{R,PZT}$ are still acceptable compared to the sensitivity of each parameter to the presence and severity of a surface-breaking crack Fig. 10.

### 4.3 Sensitivity of the Measured Surface Wave Parameters to the Depth of a Surface-Breaking Crack

Figure 10 shows the relationship between the normalized transmission coefficient of surface waves $Tr_{PZT,n}$ and the normalized crack depth, $h/\lambda$. The results in Fig. 10 were obtained from the surface wave measurements across five surface-breaking cracks with depths of 10, 20, 30, 40, and 50 mm, respectively. Shown in Fig. 10 are only twelve transmission coefficient values for each crack depth in a useful frequency range (i.e., from 20 kHz to 80 kHz with intervals of 5 kHz). Therefore, 60 dots are shown as solid circles in Fig. 10. The approximate expression that describes the relationship between $Tr_{PZT,n}$ and $h/\lambda$ is established by a non-linear regression of the experimental data as follows, and shown as a dash line in Fig. 10.

$$tr_n = 0.1515\,(h/\lambda)^{-0.7152} \qquad 0.1 \le h/\lambda \le 1.4 \qquad (4)$$

In comparison, a theoretical model obtained from a series of numerical simulations (FEM) is shown as a solid line in the same figure.

In a surface wave transmission test, many transmission values can be obtained within a frequency range; thus, multiple redundant estimates of crack depth may be calculated from a single measurement. In this study, the depth of a

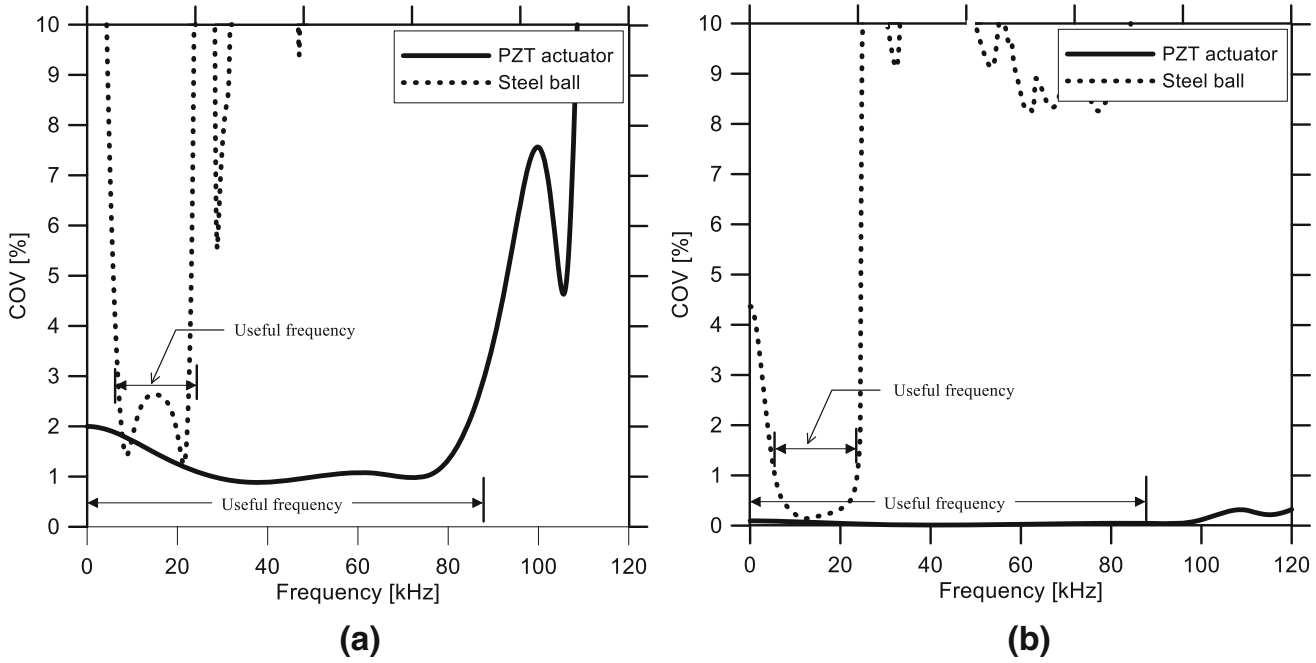


**Fig. 8** The coefficient of variation of the surface wave transmission and velocity.

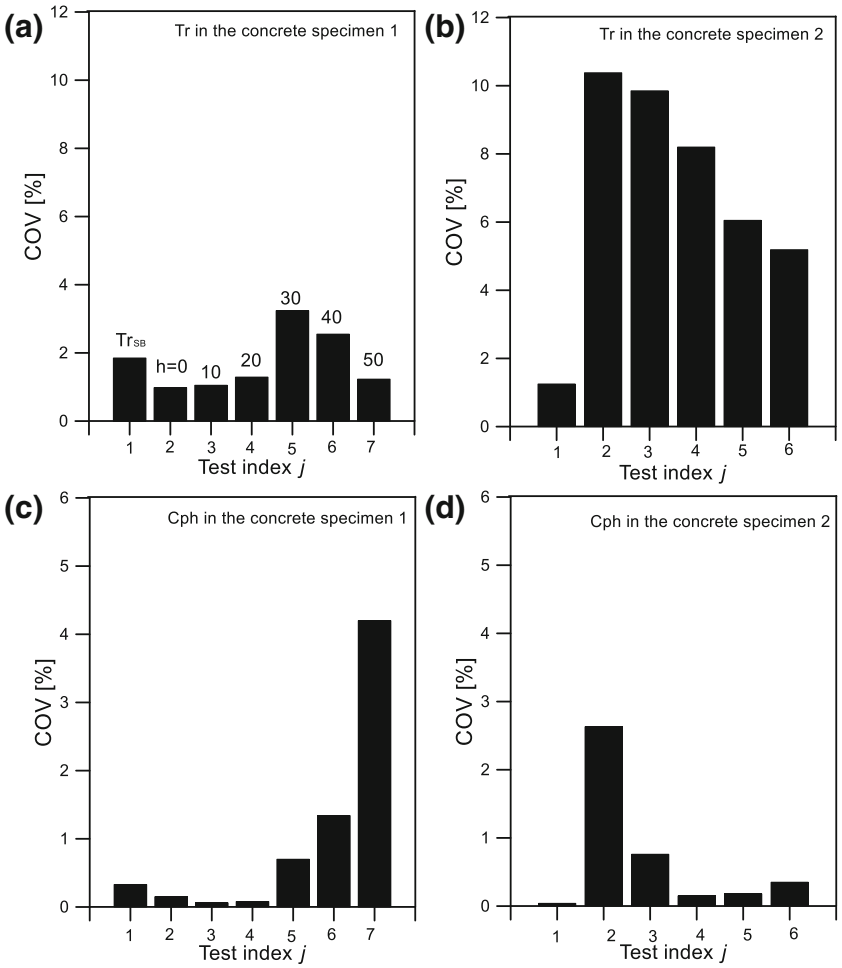


**Fig. 9** The coefficient of variation (COV) of the surface wave transmission $Tr_{PZT}$ and velocity $C_{RPZT}$: **a**, **b** COV of $Tr_{PZT}$ measured in concrete specimens 1 and 2, respectively, **b** COV of $C_{RPZT}$ measured in concrete specimens 1 and 2, respectively.

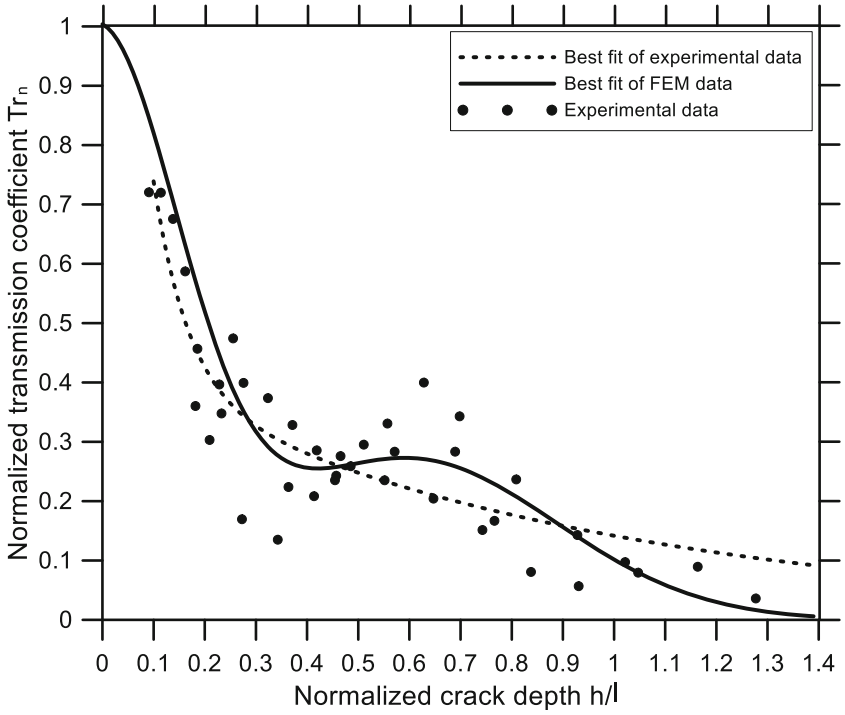


**Fig. 10** Normalized transmission coefficient $Tr_{PZT,n}$ versus normalized crack depth $h/\lambda$.

surface-breaking crack was determined by using the least square method. The optimum depth result was determined to minimize the sum of square residuals of the transmission function (SSR),

$$SSR = \sum_{i=1}^{N} \left( \frac{tr_n(f_i, h/\lambda_i) - tr'_n(f_i)}{tr_n(f_i, h/\lambda_i)} \right)^2 \quad (5)$$

where $tr_n$ is the transmission ratio in the proposed calibration curve in Eq. (4), $Tr_n$, is the measured transmission ratio calculated using Eq. (1), $i$ is an index of input values, and $f_i$ and $\lambda_i$ are the frequency and wavelength with the index $i$. As a result, the crack depths estimated for the notch-type cracks (using the surface wave transmission measurement $h_{tr}$) were 8, 18, 26, 42 and 48 mm, respectively. The estimated values are about 80–90 % compared to the as-built crack depths. Therefore, the proposed model can be effective for evaluating the depth of a surface-breaking crack in concrete.

### 4.4 Effect of Crack Depth on Surface Wave Velocity Measurement

Figure 11 shows the variation in surface wave velocity at 20 kHz with increasing crack depths obtained from numerical simulation and experiment in this study. It was observed that $C_R$ obtained from numerical simulation remains stable around the reference velocity of 2250 m/s until crack depth is less than about 120 mm. For the experimental data, the surface wave velocity at 20 kHz was 2208 m/s in the crack free-region. Increasing the crack depth up to 50 mm does not affect the surface wave velocity at 20 kHz. This observation is consistent with observations by previous researchers (Masserey and Mazza 2007) that the surface wave velocity is only sensitive to a crack deeper than about 80 % of the wavelength of surface waves. Compared to the surface wave transmission coefficient, the phase velocity is less sensitive to the presence of cracks. However, it is reasonable to say that some degradation of the surface wave velocity (about

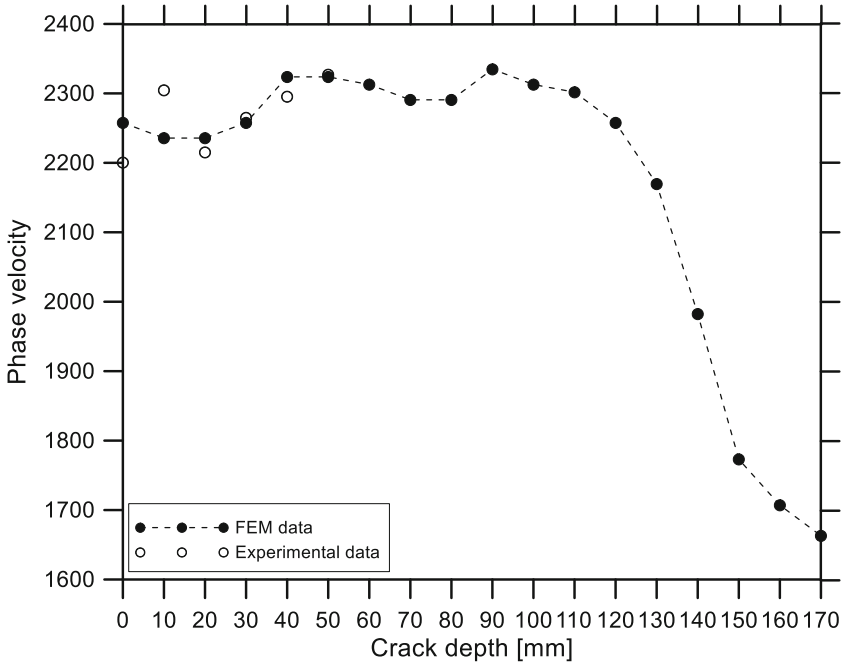


**Fig. 11** Phase velocity of surface waves $C_R$ versus crack depth $h$.

**Table 1** Loading history in test stages 1, 2, and 3 for specimen 2

| Test stage 1 | | Test stage 1 | | Test stage 1 | |
|---|---|---|---|---|---|
| Test steps $i$ | Loading $P_1$ [kips (kN)] | Test steps $i$ | Loading $P_2$ [kips (kN)] | Test steps $i$ | Loading $P_3$ [kips (kN)] |
| 0 | 0 | 7 | 1 (4.48) | 12 | 0 |
| 1 | 4 (17.79) | 8 | 2 (8.89) | 13 | 4 (17.79) |
| 2 | 8 (35.58) | 9 | 3 (13.34) | 14 | 8 (35.58) |
| 3 | 12 (53.37) | 10 | 3.5 (15.56) | 15 | 12 (53.37) |
| 4 | 16 (71.17) | 11[a] | – | 16 | 16 (71.17) |
| 5 | 20 (88.96) | | | 17 | 20 (88.96) |
| 6 | 24 (106.75) | | | 18 | 24 (106.75) |

[a] Onset of cracking.

10 %) across a surface-breaking crack is evidence of a deep crack, comparable to the wavelength of surface waves.

### 4.5 Application to Monitoring a Concrete Beam under Various Loadings

Described in this section is the application of the surface-mount sensor to concrete subjected to various loadings, which are common in actual concrete structures. Surface wave transmission and velocity were monitored in a step-wise manner in the various test steps described in Table 1. Figure 12a, b are plots illustrating the variations in the normalized transmission coefficients and phase velocity at a frequency of 20 kHz, respectively, in different test steps.

Before cracking, there was only a slight change in $Tr_n$ and $Cr_R$ with increasing compressive loadings up to 106.75 kN (24 kips). Furthermore, with increasing tensile stress up to 3 MPa (420 ksi), which corresponds to a cracking moment of the concrete specimen, both $Tr_n$ remain almost constant (±2 % of the reference $Tr_n$) until the onset of the first surface-breaking crack on the top surface of specimen 2. The crack depth measured on the side surfaces of the concrete specimen was about 120 mm, which shows close agreement with the depth measured from a core sample taken at the surface after testing (see Fig. 13). In addition, $C_R$ tends to decrease slowly with increasing compressive and bending loadings, and exhibit small variations (see Fig. 12b). Once a crack appears, $Tr_n$ and $C_R$ suddenly decrease to about 10 and 85–90 % of the reference values, respectively. It appears that $Tr_n$ is much more sensitive to the presence of a surface-breaking crack in concrete than $C_R$. In summary, monitoring $Tr_n$ and $C_R$ can be effective for identifying the onset of a surface-breaking crack in concrete, and the approximate

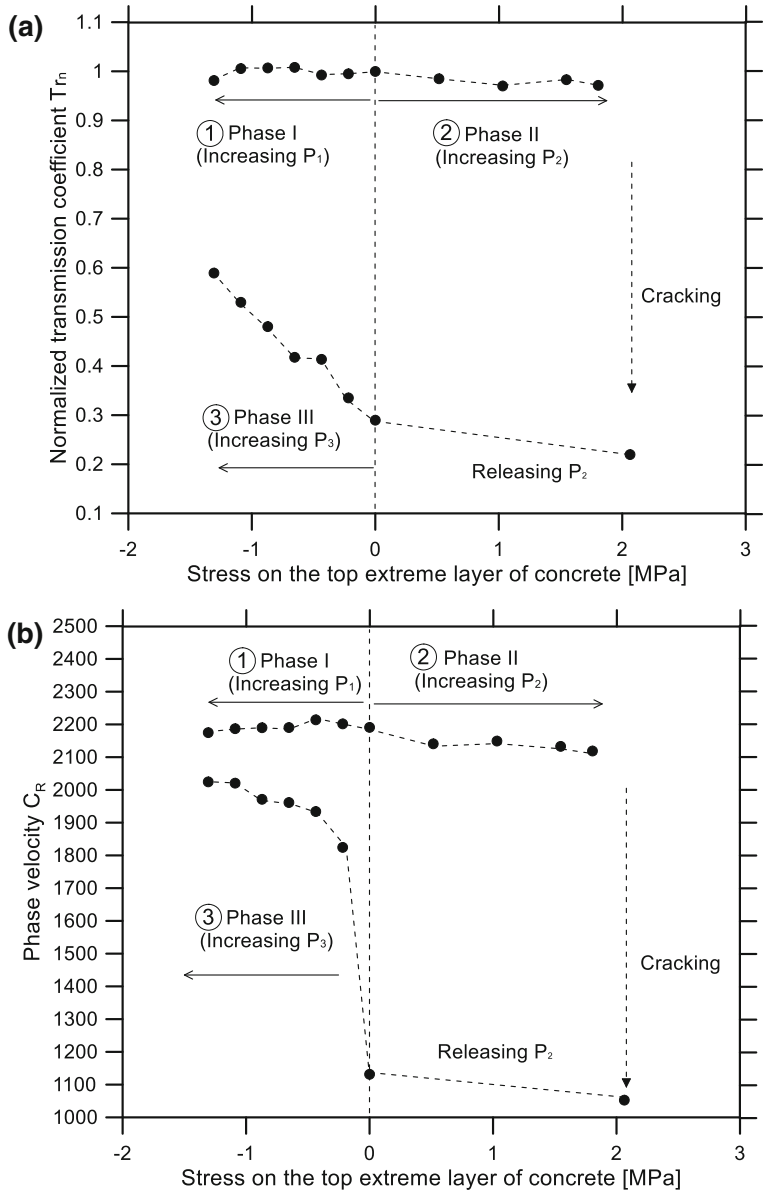


**Fig. 12** Variation of transmission coefficient and phase velocity of surface waves at 20 kHz with stress on top extreme layer of concrete: **a** normalized transmission coefficient versus stress, and **b** phase velocity versus stress.

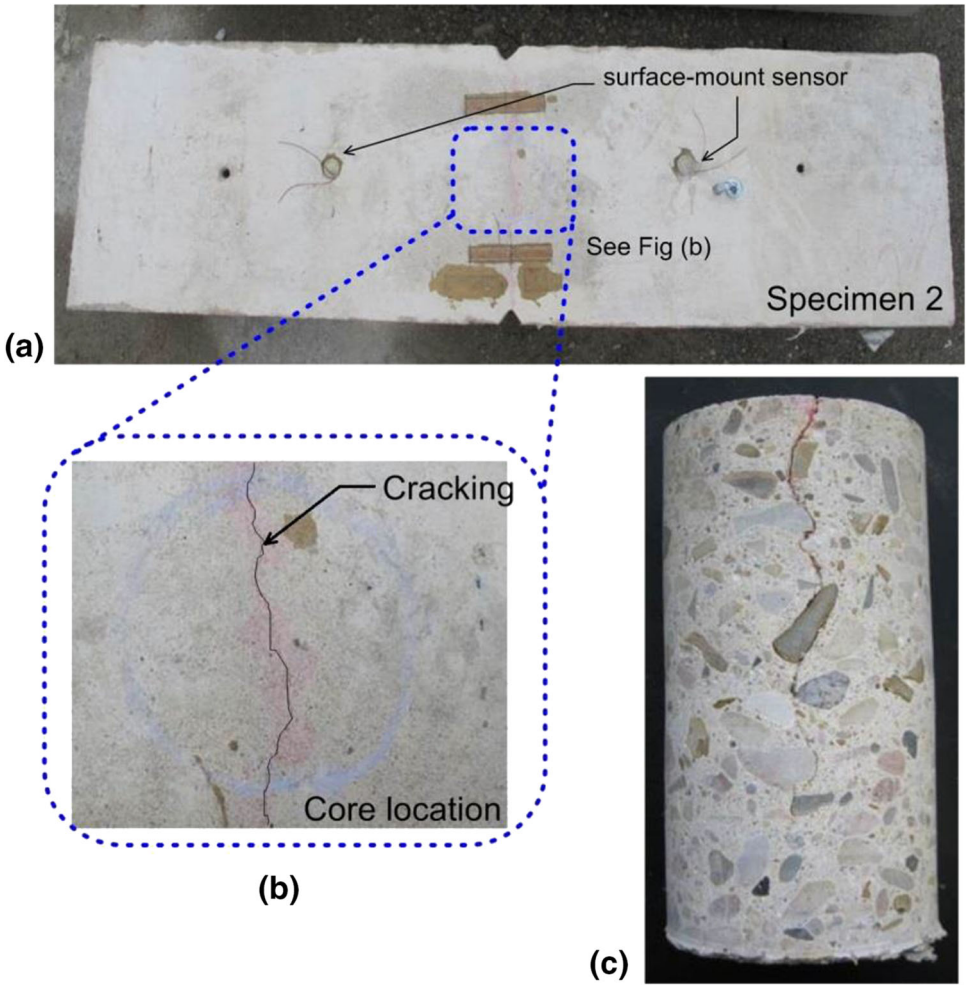


**Fig. 13** Core samples extracted after completing tests from the test specimen 2: **a** concrete specimen 2 after testing, **b** location of core extraction, and **c** core sample.

depth can be estimated by using the SWT method. In addition, this process can be automated by using surface-mount sensors.

However, the effect of external loadings may pose difficulties in the interpretation of $Tr_n$ and $C_R$. As shown in Fig. 12, $Tr_n$ and $C_R$ increase with an increase in the application of external compression $P_3$. At the last loading step of $P_3$, $Tr_n$ and $C_R$ were recovered to 90 and 95 %, respectively, of the values before cracking. Some portions of the incident surface waves (i.e., crack interfacial waves) are transmitted through the interface of an actual crack, which commonly has a partially closed interface. Increasing the compressive force gradually closes the concrete crack, increasing the interfacial stiffness of the crack. It was observed that both $Tr_n$ and $C_R$ are enhanced, owing to the crack interfacial waves, which may lead to substantial errors in predicting the depth of a surface-breaking crack in actual concrete structures.

One interesting finding is related to the potential for combining the results from the SWT and SASW as a more reliable crack depth estimation approach for testing actual structures. As observed in the theoretical results, the surface wave velocity is only sensitive to a crack deeper than about 80 % of the wavelength of surface waves. In addition, it was observed that the surface wave velocity is less sensitive to the interfacial stiffness of a surface-breaking crack than the surface wave transmission. Therefore, it is reasonable to say that some degradation of the surface wave velocity (about 10 %) across a surface-breaking crack is evidence of a deep crack, compared to the wavelength of surface waves.

## 5. Conclusions

In this paper, experimental results are presented to investigate the applicability of piezoelectric sensors as a consistent impact source for automated surface wave measurements in concrete structures. The conclusions are summarized as follows,

(1) The piezoelectric surface-mount sensors produce excellent signal coherence $\gamma \geq 0.999$ in a wideband frequency range from 0 to 120 kHz. In contrast, signals generated by manual impacts have good signal consistency in a narrower frequency range of 10–30 kHz, and are dependent on the diameter of the steel ball. It was observed that the surface-mount

sensors have consistent coupling under various stress states and damage levels of concrete.

(2) Experimental variability in the transmission and velocity measurements measured using the piezoelectric surface-mount sensors are equivalent or less than that from manual impacts. The COVs of the $Tr_{PZT100}$ and $C_{R,PZT100}$ are $1.24 \pm 0.39$ % ($\mu \pm \sigma$), and $0.04 \pm 0.023$ %, respectively, in a useful frequency range of 0–120 kHz. In contrast, the COVs of the $Tr_{SB}$ and $C_{R,SB}$ are $2.29 \pm 0.65$ % ($\mu \pm \sigma$), and $0.3 \pm 0.15$ %, respectively, in a useful frequency range of 10 kHz to 30 kHz.

(3) The proposed model for the surface wave transmission coefficient is demonstrated to be effective for evaluating the depth of a surface-breaking crack in concrete. However, special care is needed to apply the surface wave transmission method to a partially closed crack in actual concrete structure because of interference of the crack interfacial waves with transmitted surface waves.

(4) Results from experiments and numerical simulations show that the surface wave velocity is only sensitive to cracks deeper than about 80 % of the wavelength of surface waves. However, it is reasonable to say that some degradation of the surface wave velocity (about 10 %) across a surface-breaking crack is evidence of a deep crack comparable to the wavelength of surface waves. Therefore, a fusion of the results from the SWT and SASW can be used as a more reliable crack depth estimation approach for testing actual structures.

## Acknowledgments

This research was supported by a grant (15DRP-B066470-03) from Infrastructure and transportation technology promotion research Program funded by Ministry of Land, Infrastructure and Transport of Korean government.

## Open Access



## References

Achenbach, J. D. (2000). Quantitative nondestructive evaluation. *International Journal of Solids and Structures, 37*(1–2), 13–27.

Achenbach, J. D. (2002). Modeling for quantitative non-destructive evaluation. *Ultrasonics, 40*(1–8), 1–10.

Achenbach, J. D., Keer, L. M., & Mendelsohn, D. A. (1980). Elastodynamic analysis of an edge crack. *Journal of Applied Mechanics, 47*(3), 551–556.

ACI Committee 228 (1998). Nondestructive test methods for evaluation of concrete in structures. *Report ACI 228.2R-98*, American Concrete Institute, Farmington Hills, MI.

Angel, Y. C., & Achenbach, J. D. (1984). Reflection and transmission of obliquely incident Rayleigh waves by a surface-breaking crack. *The Journal of the Acoustical Society of America, 75*(2), 313–319.

ASTM C39. (2014). *Standard test method for compressive strength of cylindrical concrete specimens*. West Conshohocken: ASTM International.

Dong, B., Xing, F., & Li, Z. (2011). Cement-based piezoelectric ceramic composite and its seosor applications in civil engineeriing. *ACI Materials Journal, 108*(5), 543–549.

ElSafty, A., & Abdel-Mohti, A. (2013). Investigation of likelihood of cracking in reinforced concrete bridge decks. *International Journal of Concrete Structures and Materials, 7*(1), 79–93.

Graff, K. (1991). *Wave motion in elastic solid*. New York: Dover Publications.

Gucunski, N., Imani, A., Romero, F., Nazarian. S., Yuan, D., Wiggenhauser, H., et al. (2013). Nondestructive testig to identify concrete bridge deck deterioration. *SHRP 2 Report S2-R06A-RR-1*.

Hevin, G., Abraham, O., Petersen, H. A., & Campillo, M. (1998). Characterization of surface cracks with Rayleigh waves: A numerical model. *NDT and E International, 31*(4), 289–298.

Hou, S., Zhang, H. B., & Ou, J. P. (2012). A PZT-based smart aggregate for compressive seismic stress monitoring. *Smart Materials and Structures, 21*, 105035.

Hou, S., Zhang, H. B., & Ou, J. P. (2013). A PZT-based smart aggregate for seismic shear stress monitoring. *Smart Materials and Structures, 22*, 065012.

Jung, M. J. (2005). *Shear wave velocity measurements of normally consolidated kaolinite using bender elements*. Master of Science in Engineering, The University of Texas at Austin, Austin.

Kee, S.-H. (2011). *Evaluation of crack-depth in concrete using non-contact surface wave transmission measurement*. Doctor of Philosophy, The University of Texas at Austin, Austin, TX.

Kee, S.-H., & Zhu, J. (2010). Using air-coupled sensors to determine the depth of a surface-breaking crack in concrete. *The Journal of the Acoustical Society of America, 127*(3), 1279–1287.

Kee, S.-H., & Zhu, J. (2011). Effects of sensor locations on air-coupled surface wave transmission measurements. *Ultrasonics, Ferroelectrics and Frequency Control, IEEE Transactions on, 58*(2), 427–436.

Kee, S.-H., & Zhu, J. (2013). Using piezoelectric sensors for ultrasonic pulse velocity measurements in concrete. *Smart Materials and Structures, 22*(11), 115016.

Liao, W. I., Wang, J. X., Song, G., Gu, H., Olmi, C., Mo, Y. L., et al. (2011). Structural health monitoring of concrete columns subjected to seismic excitations using piezoceramic-

based sensors. *Smart Materials and Structures, 20*(12), 125015.

Masserey, B., & Mazza, E. (2007). Ultrasonic sizing of short surface cracks. *Ultrasonics, 46*(3), 195–204.

McLaskey, G. C., & Glaser, S. D. (2010). Hertzian impact: Experimental study of the force pulse and resulting stress waves. *Journal of the Acoustical Society of America, 128*(3), 1087–1096.

Mendelsohn, D. A., Achenbach, J. D., & Keer, L. M. (1980). Scattering of elastic waves by a surface-breaking crack. *Wave Motion, 2*(3), 277–292.

Nazarian, S., & Desai, M. R. (1993). Automated surface wave method: Filed testing. *Journal of Geotechnical Engineering, ASCE, 119*(7), 1094–1111.

Nazarian, S., & Stokoe, K. H., II (1986). In-situ determination of elastic moduli of pavement systems by spectral-analysis-of-surface-wave method (practical aspects). *Research Report 368-1F*, University of Texas at Austin, Center for Transportation Research.

Okafor, A. C., Chandrashekhara, K., & Jiang, Y. P. (1996). Delamination prediction in composite beams with built-in piezoelectric devices using modal analysis and neural network. *Smart Materials and Structures, 5*(3), 338–347.

Popovics, J. S., Song, W.-J., Ghandehari, M., Subramaniam, K. V., Achenbach, J. D., & Shah, S. P. (2000). Application of surface wave transmission measurements for crack depth determination in concrete. *ACI Materials Journal, 97*(2), 127–135.

Shin, S. W., Zhu, J., Min, J., & Popovics, J. S. (2008). Crack depth estimation in concrete using energy transmission of surface waves. *ACI Materials Journal, 105*(5), 510–516.

Soltani, A., Harries, K. A., & Shahrooz, B. M. (2013). Crack opening behavior of concrete reinforced with high strength reinforcing steel. *International Journal of Concrete Structures and Materials, 7*(4), 253–264.

Song, G. B., Gu, H. C., & Mo, Y. L. (2008). Smart aggregates: multi-functional sensors for concrete structures—a tutorial and a review. *Smart Materials and Structures, 17*(3), 033001.

Song, G., Gu, H., Mo, Y. L., Hsu, T. T. C., & Dhonde, H. (2007). Concrete structural health monitoring using embedded piezoceramic transducers.". *Smart Materials and Structures, 16*(4), 959–968.

Song, G., Mo, Y. L., Otero, K., & Gu, H. (2006). Health monitoring and rehabilitation of a concrete structure using intelligent materials. *Smart Materrials & Structures, 15*(2), 309–314.

Song, W.-J., Popovics, J. S., Aldrin, J. C., & Shah, S. P. (2003). Measurement of surface wave transmission coefficient across surface-breaking cracks and notches in concrete. *The Journal of the Acoustical Society of America, 113*(2), 717–725.

Wang, C. S., Wu, F., & Chang, F. K. (2001). Structural health monitoring from fiber-reinforced composites to steel reinforced concrete. *Smart Materials and Structures, 10*(3), 548–552.